J Mater Sci (2009) 44:365–373
DOI 10.1007/s10853-008-3152-6

Mechanical properties and strain fatigue lives of insulation polymers

Shing-Chung Wong · Sunil Bandaru

Received: 5 September 2008 / Accepted: 2 December 2008 / Published online: 16 December 2008

Abstract Insulation polymers are not well characterized for their mechanical properties particularly in terms of fatigue strains. This article aims to examine the durability and strain fatigue lives of three commonly used cable insulation polymers, viz., (1) polyvinyl chloride (PVC), (2) crosslinked polyethylene (XLPE), and (3) polyphenylene ether (PPE) under selected strain and temperature ranges. The tensile properties of these materials were measured using an Instron testing machine at constant and controlled loading rates. Fatigue tests were performed at three selected temperatures, −40, 25, and 65 °C, to characterize the temperature effects on fatigue life. From the tensile test results, it was observed that PVC and XLPE are ductile and exhibit significantly more elongation prior to breaking, while PPE exhibits brittle behavior. When the loading rate is increased, there is an improvement in the tensile strength of PPE and elastic modulus of PPE and PVC. The durability of XLPE under strain fatigue testing was the largest, followed by PVC and PPE. The strain fatigue lives of PVC and XLPE decreased drastically at −40 °C and demonstrated a noted increase at 65 °C compared to fatigue lives at room temperature. This trend was not observed in PPE where the strain fatigue life showed improvement at both lower and higher temperatures.

Introduction

Cable insulation plastics are a unique set of polymers that are not well understood for their strain fatigue lives [1]. Wiring/cable harness is a system in which individual bundles of cables/wires are bound together by clamps, cable ties, sleeves, electrical tape, etc. This enables easy installation and maintenance and also secures them against the adverse effects of vibration, abrasion, and moisture. Polyvinyl chloride (PVC), crosslinked polyethylene (XLPE), and polyphenylene ether (PPE) are the principal insulation materials used in the wire-harnessing industry [2–12]. They constitute insulation and jacketing functionality for different types of cable and wire products.

PVC is a thermoplastic material widely used as insulations for cable harnessing primarily because of its excellent electrical and thermal insulation properties, durability, flexibility, and ease of handling in installation [13, 14]. XLPE obtained by crosslinking PE has improved thermal stability and mechanical properties. Its superior thermal resistance and electrical properties render it the material of choice for cables [5, 6]. PPE, an engineering thermoplastic, has excellent properties such as high strength, high dimensional stability, and low moisture uptake [15–22]. The high glass transition temperature, T_g, of PPE makes it ideal for electrical and automotive equipment that is continuously exposed to high temperatures [23]. With the addition of plasticizers, the T_g can be reduced which helps in increasing flexibility and processing at low temperatures [24, 25].

Engineering thermoplastic materials can sustain large deformation after necking during tensile testing. This has been observed in the case of polyethylene (PE) [26–32], polypropylene (PP) [30–32], rubber-toughened polystyrene [33], polycarbonate (PC) [32, 34, 35], and its alloys [36]. This behavior of thermoplastic materials is advantageous to the manufacturing process and mechanical performance but presents a challenge when attempting to model such behavior. The development of a strain fatigue model,

S.-C. Wong (✉) · S. Bandaru
Department of Mechanical Engineering, The University of Akron, Akron, OH 44325-3903, USA
e-mail: swong@uakron.edu

which is attempted in this research, for large deformation behavior of polymeric materials lags far behind that for metallic materials [37].

True stress–true strain behavior is one of the most fundamental properties of a structural material. Extensive research over the past two decades on polymers has shown the importance of true stress–true strain curves in providing useful information about the yielding behavior, the true rate of strain hardening, and the stress-induced transformations of crystalline phases within the polymer [32, 38, 39]. Furthermore, true stress–true strain behavior can be used in the development of constitutive relationships and finite element models to accurately predict multi-axial stress states in complex geometries.

The cables in the wire harnessing are periodically exposed to external loading which includes torsion and bending. Following these mechanical loads, the life is limited due to the internal failures initiated by cyclic deformation, fatigue and wear of internal conductors. For this reason, better understanding of the static and dynamic behaviors of polymers under given loading conditions is desired [40]. The results are essential for comparing the risks of mechanical failures occurring in insulation polymers.

In this article, we present the true stress–true strain relationships and the extremely useful strain fatigue lives of three commonly used insulation plastics, namely, PVC, XLPE, and PPE. Such results are presently lacking and they will be reported herein as functions of selected frequency and temperature ranges.

Experimental work

Materials

The polymers used in this study are PVC, XLPE, and PPE in the form of pellets. The average specific gravities at room temperatures for PVC, XLPE, and PPE are 1.28, 1.42, and 1.04 g/cm^3, respectively, in accordance with ASTM Standard D-792. Therefore, PPE has the lowest specific gravity among the three, to be followed by PVC and XLPE.

Specimen preparation

Prior to molding, all the pellets were dried at 60 °C under vacuum for 24 h. The dried pellets of PVC and PPE were injection molded into ASTM 638D standard dogbone specimens using a Vandorn 55 injection-molding machine. The temperatures in the barrel and mold were maintained at 160 °C (320 °F) and 26.7 °C (80 °F), respectively, for PVC and 288 °C (550 °F) and 76.7 °C (170 °F) for PPE. XLPE could not be injection molded because of the rapid crosslinking, which generated too high a viscosity during plasticating. Compression molding of XLPE was carried out using compression molding press by Carver Inc. Both top and bottom mold temperatures were maintained at 129 °C (265 °F) and a pressure of 4000 psi was applied for 20 min to produce rectangular sheets of 3.5 mm thickness. These sheets were cut into standard dogbone specimens using a specially designed press and punch die cutter in our laboratory.

Thermogravimetric analysis

TGA was conducted to assess the thermal degradations of PVC, XLPE, and PPE. The TGA 2050 from TA Instruments was used. Change in the weight of the polymers as a function of temperature is determined using this method. Nitrogen was used for purging with flow rates of 10 and 90 mL/min, respectively. The temperatures ranged from 25 to 600 °C at a ramping rate of 30 °C/min. The sample weight was maintained in the range of 2–5 mg. The thermal stability results are summarized in Table 1.

Dynamic mechanical analysis

Dynamic mechanical analysis (DMA) was employed to measure the viscoelastic properties of the studied materials. DMA was also used for the determination of glass transition temperatures. Rectangular strips were cut with 20 mm in length and 10 mm in width from the tensile specimens. The thickness of the PVC and XLPE samples was 3.06 mm while the PPE sample was cut from a 1-mm-thick slab because PPE was significantly stiffer than PVC and XLPE. A Perkin Elmer DMA was used at a frequency of 10 Hz in the tensile mode. Storage modulus (E'), loss modulus (E''), and loss tangent delta (tan δ) were measured between −60 and 100 °C at a ramping rate of 4 °C/min and a sampling interval of 0.05 s. Nitrogen flow was set at a pressure of 40 psi and circulated in the furnace during the experiments. Liquid N_2 was supplied for cooling.

Table 1 Summary of thermal stability results of PVC, XLPE, and PPE

Material	Thermal degradation temperature (°C)	Mass loss at 500 °C (%)
PVC	267.6	83
XLPE	298.0	60
PPE	402.0	77

Tensile tests

In order to determine the true stress–true strain relationships, we seek to measure full-field displacements and strains in all three dimensions with the help of two mechanical contact extensometers. Volumetric strain data obtained provide valuable insight into the mechanisms of deformation.

Uniaxial tensile tests were conducted using a quasi-static Instron 5582 with a load cell of 10 kN at 25 °C. A set of specimens of each material were loaded at selected loading rates from 5 to 60 mm/min to examine the variation of mechanical properties with loading rate. Two mechanical contact extensometers were mounted at the center of specimen to measure strains induced in the sample in both longitudinal and transverse directions. The photograph of the setup is shown in Fig. 1. With these high-precision extensometers it is possible to determine elastic modulus and Poisson's ratio at different loading rates. The true stress, σ, of each sample was obtained from [41]

$$\sigma = P/\left[W_o T_o (1-\varepsilon_z)^2\right] \quad (1)$$

where P is the applied load, W_o and T_o are the original width and thickness, respectively. The true strain ε_z is directly obtained from the transverse extensometer.

Many polymers increase in volume during tensile extension. Volumetric strain is important to measure because it is a key macroscopic indicator of microscopic processes. Small-scale internal fracture processes such as crazing (glassy polymers) or crystal fragmentation (semi-crystalline polymers) are manifested by volumetric strain [29]. Unlike metals, the Poisson's ratio for polymeric materials decreases from an initial value of 0.4 to about 0.2–0.3 with an increase in uniaxial deformation [42].

The volumetric strain [41], also known as dilatational strain [43], is obtained by

$$\Delta V/V = (1+\varepsilon_x)(1+\varepsilon_z)^2 - 1 \quad (2)$$

Table 2 Values of the slopes of volumetric strain versus longitudinal strain for PVC, XLPE, and PPE

Loading rate (mm/min)	PVC	XLPE	PPE
5	1.64	1.64	1.76
10	1.60	1.59	1.47
15	1.63	1.58	1.58
20	1.60	1.40	1.32
25	1.57	1.60	1.40
30	1.65	1.58	1.85
40	1.53	1.55	1.76
50	–	1.64	1.38
60	–	1.55	1.65

where ε_x denotes the strain in the loading direction and ε_z denotes the strain in the lateral direction. Table 2 shows the values of the slopes of the volumetric strain versus longitudinal strain curves with varying loading rates.

A set of tensile tests were conducted separately to examine the tensile strength, breaking strain and their variation with loading rates for each material. These tests are done without extensometers and the results are tabulated in Tables 3 and 4.

Fatigue tests

Fatigue tests were performed under displacement control on the tensile specimens using a fully automated, closed loop, servo-hydraulic mechanical testing machine (Instron model 8500) at a frequency of 5 Hz for PVC and XLPE, and 2 Hz for PPE. The different frequencies chosen are necessary to generate useful data within a reasonable time frame, i.e., 1–2 days for each sample. Fatigue data for a minimum of three specimens of each material were obtained at −40, 25, and 65 °C. The experiments were conducted considering the limitations of the servo-hydraulic machine in use. The maximum frequency that the

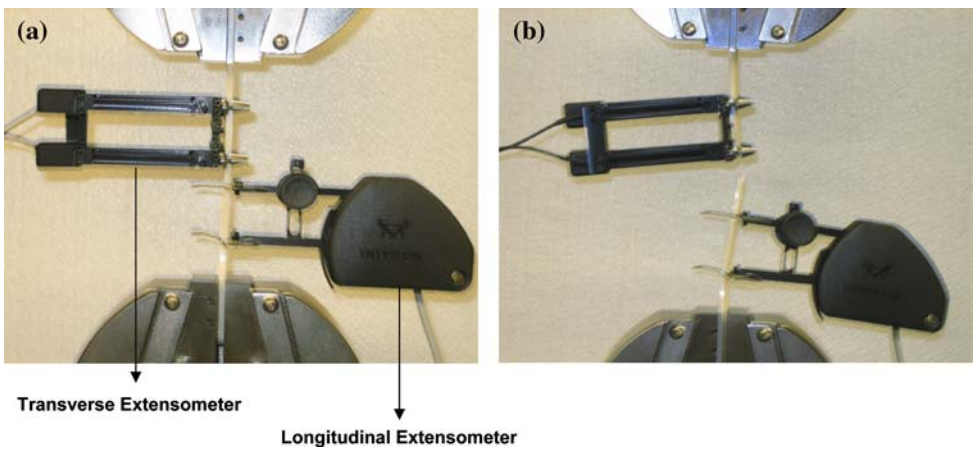

Fig. 1 **a** Photograph showing transverse and longitudinal extensometers are mounted on the centre of the specimen to measure the strains in the transverse and longitudinal directions. **b** The specimen breaks

Table 3 Average tensile strength and breaking strain values for PVC, XLPE, and PPE strained at a loading rate of 20 mm/min

Material	Tensile strength (MPa)	Breaking strain (%)
PVC	12.9	230
XLPE	10.9	224
PPE	43.8	62

Table 4 Tensile strength values at different loading rates PVC, XLPE, and PPE

Loading rate (mm/min)	PVC (MPa)	XLPE (MPa)	PPE (MPa)
5	–	10.7	42.4
10	12.7	10.1	43.7
15	13.3	10.1	44.6
20	12.8	10.9	44.8
25	12.2	9.9	45.3
30	13.0	9.6	45.3
40	12.8	10.0	46.0
50	–	9.9	46.6
60	–	10.2	46.5

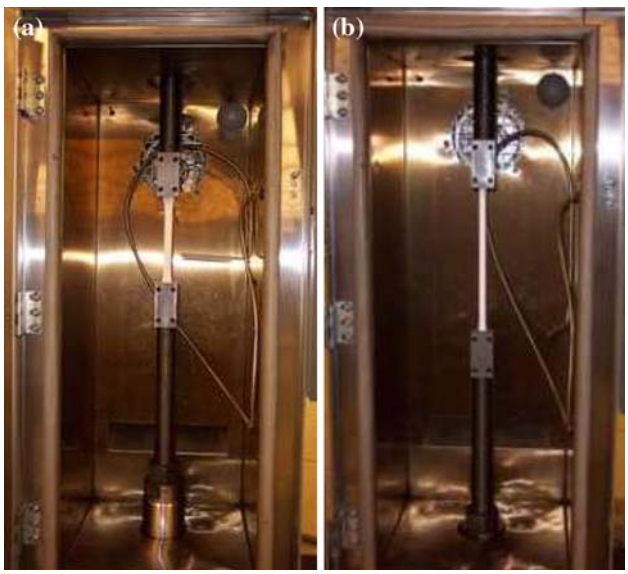

Fig. 2 The temperature box and experimental setup for fatigue tests. **a** Sample mounted between the grips prior to fatigue straining. **b** The specimen is pre-strained before applying cyclic displacements

machine can run is 5 Hz and a maximum cyclic displacement of 2.54 mm can be applied.

The experimental setup for this project required a specific design for the testing apparatus, since the testing of the samples had to be conducted at both low and high temperatures. A threaded rod is machined to form D-shaped holders to ensure a tight grip on the specimen and a full tensile loading of the specimen. Moreover, a compact

Table 5 Summary of the different strain values applied on PVC during fatigue testing

Min. strain (%)	Mean strain (%)	Max. strain (%)	Displacement (mm)	N_f (Cycles)
At −40 °C				
3.8	6.3	9.0	2.0	990
1.4	3.3	5.2	1.5	5,500
0.4	1.6	2.8	1.5	27,000
At 25 °C				
111.2	115.6	120.0	5.6	4,400
77.0	82.5	88.0	5.6	32,000
79.0	82.5	86.0	3.5	80,000
80.0	82.5	85.0	2.8	300,000
At 65 °C				
381	387	393	4.58	12,000
384	387	390	3.08	450,000
260	265	270	4.58	950,000

Table 6 Summary of the different strain values applied on XLPE during fatigue testing

Min. strain (%)	Mean strain (%)	Max. strain (%)	Displacement (mm)	N_f (Cycles)
At −40 °C				
10.0	16.5	23.0	5.1	650
9.3	13.2	17.1	3.0	7,600
8.80	11.9	15	2.3	22,000
At 25 °C				
216	220	224	5.1	25,000
172	176	180	5.1	550,000
52	56	60	5.1	1,010,000
At 65 °C				
1160	1180	1200	5.1	6,500
1020	1032	1044	3.1	198,000
952	960	970	2.0	750,000

sealed test chamber is used to control the test temperature and a compact grip design is required to fit within the limited space. Figure 2 shows a picture of a fully assembled grip setup, with sample, ready for testing. Specimens are fixed in the grips and allowed to cool (or heat) for 30 min ensuring a constant and uniform temperature distribution. Cooling is done by pumping a controlled stream of vaporized liquid nitrogen and heating is done by a heated fan on the back of the chamber.

With the exception of PPE, both PVC and XLPE have high breaking strain values. The specimens are therefore pre-strained before applying a constant amplitude cyclic displacement to enable failure within reasonable time

Table 7 Summary of the different strain values applied on PPE during fatigue testing

Min. strain (%)	Mean strain (%)	Max. strain (%)	Displacement (mm)	N_f (Cycles)
At −40 °C				
6.2	12.6	19.0	5.1	40
1.2	5.1	9.0	3.1	5,800
0.7	3.6	6.5	2.3	25,000
At 25 °C				
0.5	4.7	8.9	6.9	220
0.1	2.3	4.5	3.3	8,200
0.2	1.6	3.0	2.3	22,000
0.1	1.3	2.5	1.9	70,000
At 65 °C				
0.7	3.4	6.1	3.6	6,700
1.0	2.4	3.8	1.8	42,000
0.8	1.9	3.0	1.5	125,000

frame. The amount of pre-strain applied is equal to the mean strain. The mean strains shown in Tables 5, 6, and 7 indicate the amount of pre-strains applied to the samples. Frequency, displacement, waveform, maximum, minimum, and mean displacements are recorded.

Results and discussions

Thermogravimetric analysis

Thermogravimetric analysis (TGA) is done to check that processing did not induce severe thermal degradation in the material. It assesses mass loss as temperature increases. Figure 3 shows the comparison of TGA before and after processing for PVC, XLPE, and PPE, respectively. The degradation temperature is taken as temperature at 5% mass loss. Hence, the degradation temperatures for PVC, XLPE, and PPE are found to be 267.6, 298.0, and 402.0 °C, respectively, which implies that PPE possesses higher thermal stability, to be followed by XLPE and PVC. As indicated in Table 1, at a temperature of 500 °C, mass losses of 83, 60, and 77% were observed for PVC, XLPE, and PPE, respectively. It follows that the major mass loss of 64% is observed at 260–350 °C in the case of PVC and a mass loss of 76% in the temperature range of 400–500 °C in the case of PPE. Mass loss is observed in the case of XLPE in two steps: 18% in the temperature range from 250 to 370 °C and 44% in the range 370–500 °C. Finally, comparison of TGA results of pellets with samples obtained through processing indicates that there is a minimal molecular degradation arising from the processing conditions in the three cases.

Glass transition temperatures

Figures 4 and 5 illustrate the variation of tan δ and storage modulus as a function of temperature for PVC, XLPE, and PPE. The glass transition temperature (T_g) values of PVC, XLPE, and PPE are around 60, 4, and 180 °C, respectively, as shown by the tan δ peak at that temperature in Fig. 4. The glass transition temperature varies widely with the addition of plasticizers, blending, processing conditions and it is difficult to compare with literature values for pure polymers. From Fig. 5, we can infer that PPE exhibits superior storage modulus.

True stress and true strain relationships

The true stress–true strain curves for each of the studied materials were obtained by conducting tensile tests at selected loading rates from 10 to 60 mm/min with extensometers mounted as explained in the experimental work. PVC and XLPE show considerable elongation at break compared to PPE and the extensometers need to be removed prior to complete failure of PVC and XLPE. Figures 6, 7, and 8 show true stress–true strain relationships of PVC, XLPE, and PPE. Due to the low ductility, the extensometers can be clipped on PPE until failure. The elastic modulus is measured from the initial deformation region of true stress–true strain curve. The elastic modulus variation with different crosshead speeds is shown in Fig. 9. Clearly, PPE is significantly stiffer than PVC, followed by XLPE. Figure 10 shows the representative volumetric strain–longitudinal strain curves for each of the materials. From the results in Table 2, it is clear that the three materials show considerable amount of volumetric expansion with the increase in longitudinal strain. This suggests there should be a strong dilatational deformation mechanism such as crazing, voiding, or crystal fragmentation occurring during initial loading.

The Poisson's ratios of PVC, XLPE, and PPE are obtained from the slopes of transverse strain versus longitudinal strain curves and they are 0.2, 0.2, and 0.3, respectively. These values are highly reproducible and they are independent of the applied loading rates. The results will be useful for our future modeling efforts in understanding the strain fatigue lives of these polymers.

Strain fatigue results

The purpose of the displacement controlled fatigue tests is to produce fruitful information and insight into the influence of strain amplitude on fatigue lives of insulation polymers. At a low level of applied strain amplitude, the polymers can be cyclically loaded indefinitely within our laboratory time constraints. Due to the limitations imposed

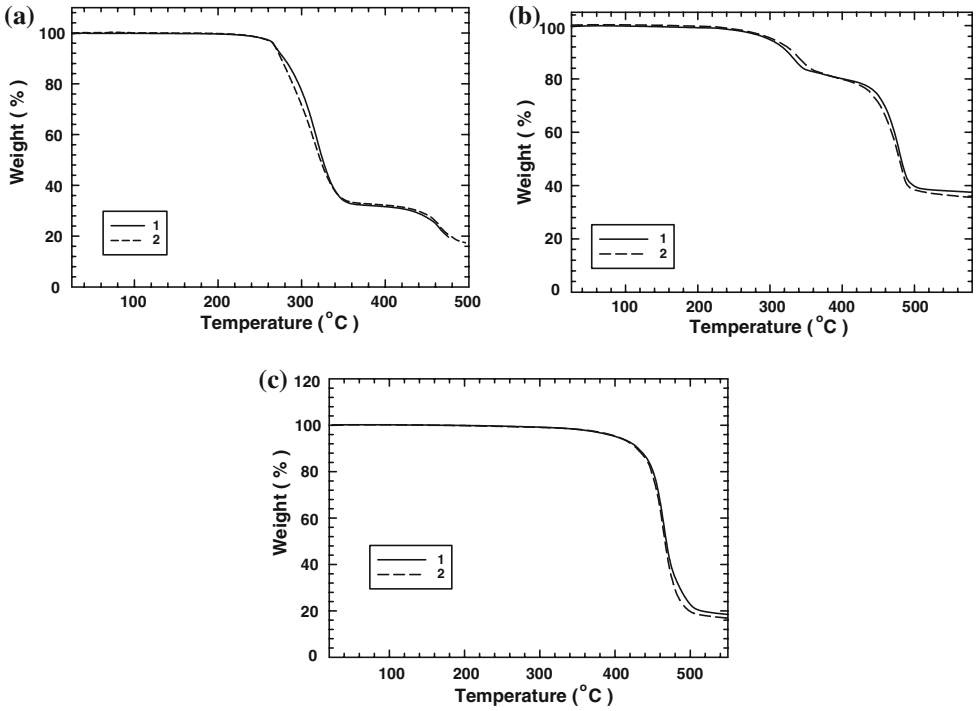

Fig. 3 TGA curves of **a** PVC, **b** XLPE, and **c** PPE. Curve "1" represents sample taken from pellets before processing; curve "2" represents sample taken from molded specimen. The comparison of the two TGA curves shows that there is minimal molecular degradation caused by the processing conditions

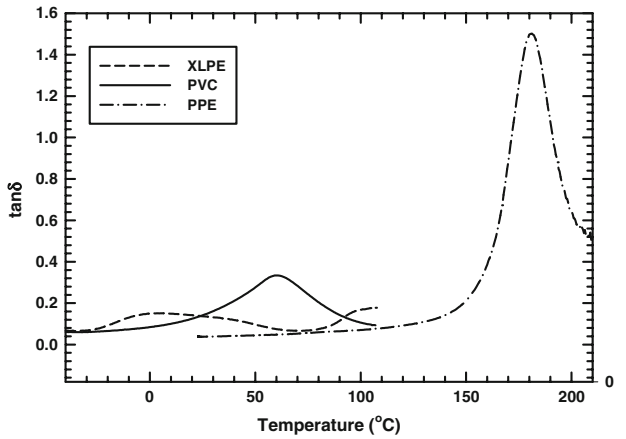

Fig. 4 The tan δ versus temperature in DMA tests for XLPE, PVC, and PPE, respectively. Note that PPE ($T_g \sim 180$ °C) requires a run at a higher temperature due to its high glass transition temperature

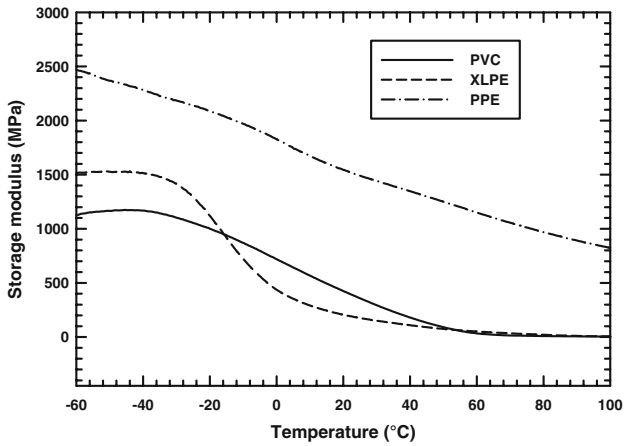

Fig. 5 Curves that represent the storage moduli, E', as a function of temperature for PVC, XLPE, and PPE. Generally, E' decreases as temperature increases

by the test time required for testing, an arbitrary cut-off value of 10^6 cycles was used to establish the endurance limit. The tests in the cold temperature are limited to around 25,000 cycles due to limited supply of liquid nitrogen.

Figures 11, 12, and 13 show a semi-log plot (3 data points each) of the maximum strain versus the number of cycles to failure for all the three materials tested at three different temperatures: −40, 25, and 65 °C. A power law curve fitted through the data indicates the characteristic trend of each sample. From the common trend we observe that at a given temperature the fatigue life increases with a decrease in maximum strain applied in the cases of all three materials. From Tables 5, 6, and 7 we observe that at a lower temperature the tested specimen accommodates lower strains, while at a higher temperature the tested specimen accommodates much higher strains compared to room temperature in the cases of PVC and XLPE. This is because when temperature is decreased most polymers go through a "ductile-brittle transition" whereby relaxation is constrained. As a result, mechanisms of deformation such as shear yielding are restricted and the polymers become brittle. At higher temperatures, the long chain molecules are able to slither over one another. Shear yielding is

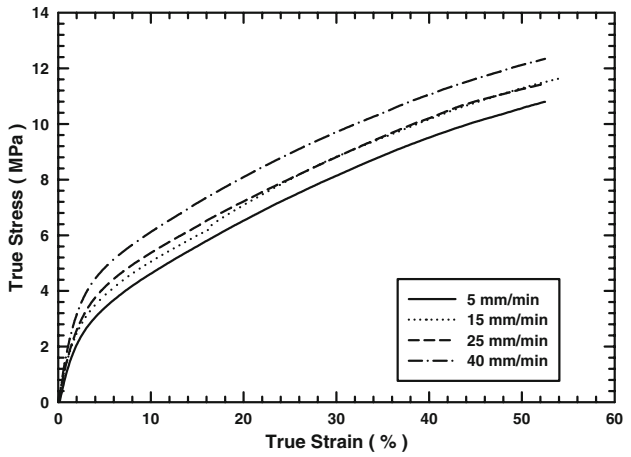

Fig. 6 True stress–true strain curves for PVC. Specimens were loaded at different crosshead speeds with extensometers to measure both the transverse and longitudinal strains. Curves for the specimens tested at 5, 15, 20, and 40 mm/min crosshead speeds are shown in the figure. The elastic moduli of these specimens are found to be 118.5, 122.4, 132.2, and 167.2 MPa, respectively

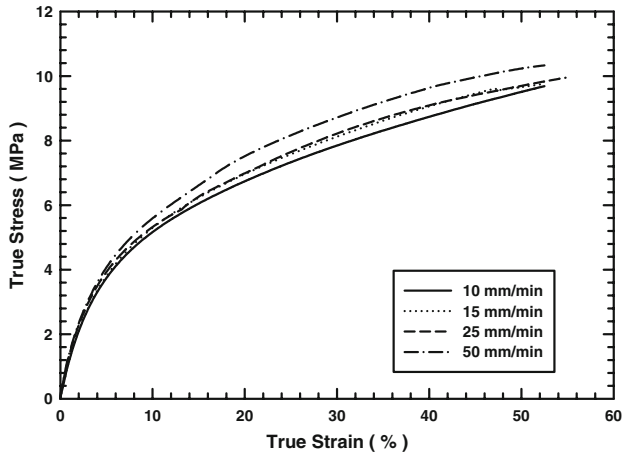

Fig. 7 True stress–true strain curves for XLPE. Specimens were loaded at different crosshead speeds with extensometers to measure both the transverse and longitudinal strains. Curves for the specimens tested at 5, 15, 25, and 50 mm/min crosshead speeds are shown in the figure. The elastic moduli of these specimens were found to be 100, 104, 108, and 108 MPa, respectively

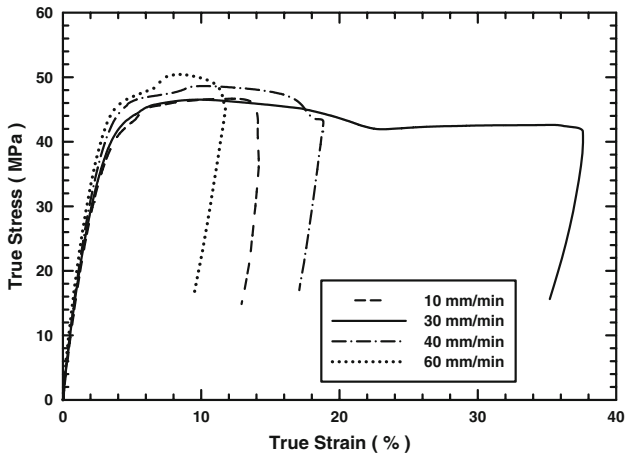

Fig. 8 True stress–true strain curves for PPE. Specimens were loaded at different crosshead speeds with extensometers to measure both the transverse and longitudinal strains and tested until failure. Curves for the specimens tested at 10, 30, 40, and 60 mm/min crosshead speeds are shown in the figure. The elastic moduli of these specimens were found to be 1.45, 1.56, 1.57, and 1.64 GPa, respectively

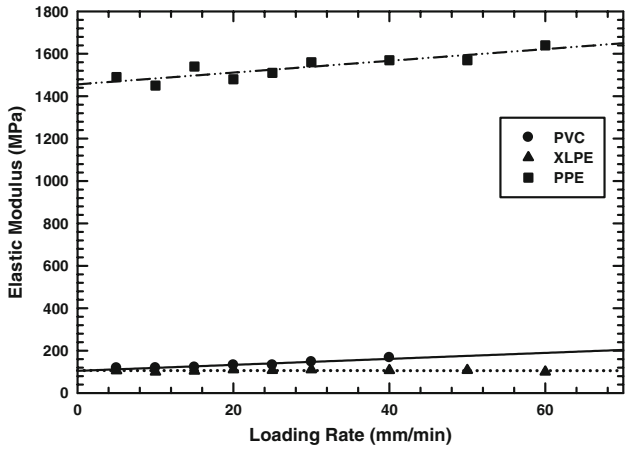

Fig. 9 The effect of loading rate on the elastic modulus of PVC, XLPE, and PPE. PPE and PVC demonstrate a steady rise in elastic modulus as the loading rate increases while no observable increase is found in XLPE

favored and the polymers become flexible. Interestingly, for PPE at both lower and higher temperatures (−40 and 65 °C), the specimens show improvement in fatigue life compared to room temperature. This by no means appears to be an anomaly due to the intrinsically brittle nature of PPE and the high T_g (180 °C) observed. As common in reinforced brittle polymers, deformation mechanisms become unique in extreme temperature ranges [44–47] and in particular for PPE below its glass transition temperature. This observation is well studied in the Friedrich's microstructural efficiency concept [47]. In many instances, intrinsically brittle polymers become more ductile at low temperatures as the craze resistance, which is thermally sensitive, decreases in comparison to the level at room temperature. As a result, conditions for crazing become favorable and the fatigue resistance of the polymer is thereby enhanced by craze formation and coalescence. The examination of the fatigue failure mechanisms is beyond the scope of the present study.

Conclusions

Three commonly used insulation polymers, viz., PVC, XLPE, and PPE, were studied for their mechanical properties and strain fatigue lives. PVC and XLPE are ductile

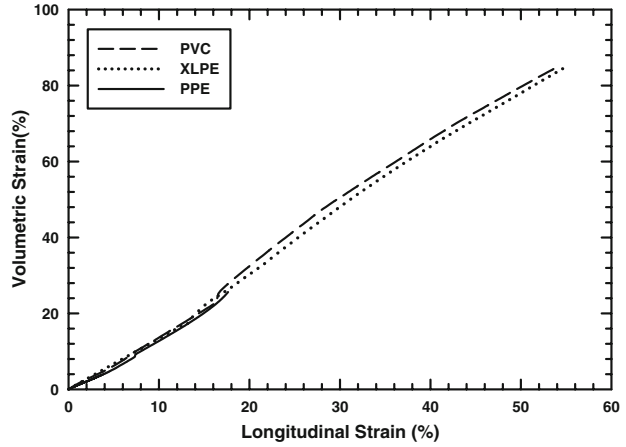

Fig. 10 Representative volume strain versus longitudinal strain curves for PVC, XLPE, and PPE. All three materials show dilatational deformation mechanisms as noted from the steep rise of the volume strain

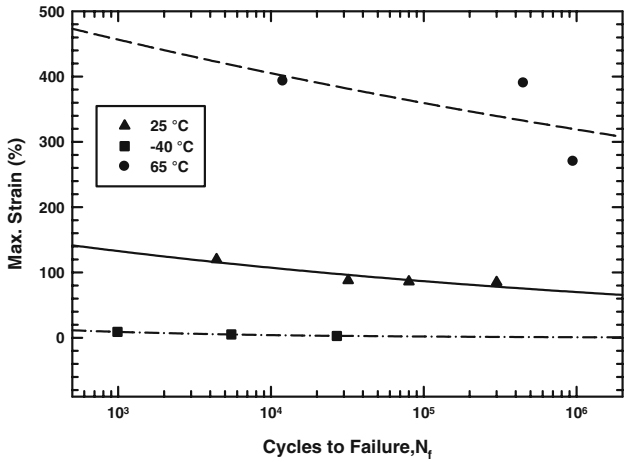

Fig. 11 Maximum fatigue strain versus the number of cycles to failure for PVC in the controlled temperature ranges

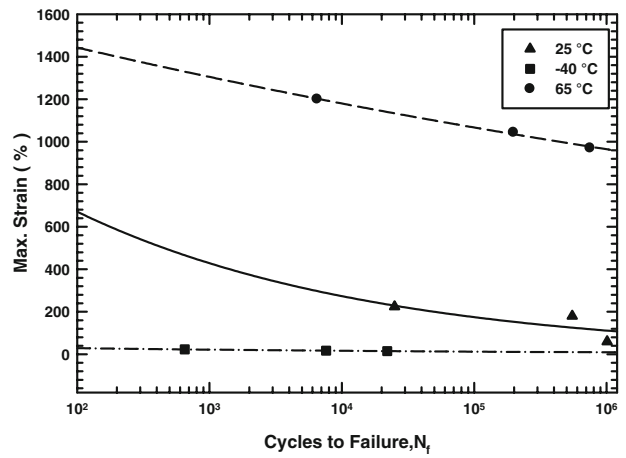

Fig. 12 Maximum fatigue strain versus the number of cycles to failure for XLPE in the controlled temperature ranges

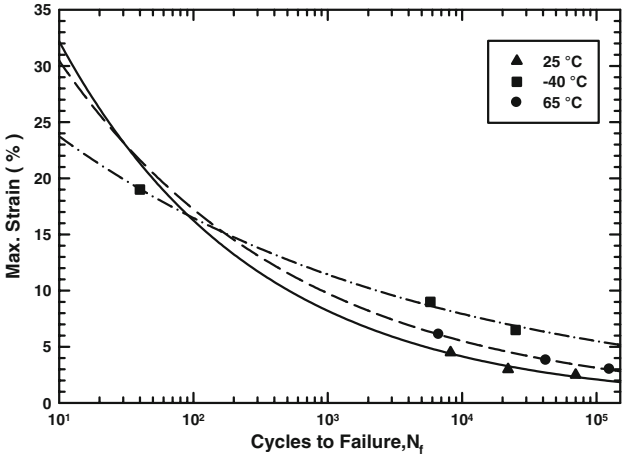

Fig. 13 Maximum fatigue strain versus the number of cycles to failure for PPE in the controlled temperature ranges

and exhibit significantly more elongation prior to breaking, while PPE exhibits brittle behavior. When the loading rate is increased, there is an improvement in the tensile strength of PPE and elastic modulus of PPE and PVC. The maximum strain versus number of cycles to failure was plotted for each of the studied materials. The durability of XLPE under strain fatigue testing was the largest, followed by PVC and PPE. The strain fatigue lives of PVC and XLPE decreased drastically at −40 °C and demonstrated a noted increase at 65 °C compared to fatigue lives at room temperature. Such an observation is consistent with the widely observed ductile-brittle transitions in polymers undergoing shear deformation. This trend was not observed in PPE where the strain fatigue life showed improvement at both lower and higher temperatures. It is conjectured that the intrinsically brittle PPE exhibited a lower craze resistance at −40 °C in comparison to that at room temperature.

Acknowledgement SCW thanks the ASEE Summer Faculty Program and R. Andrew McGill at the U.S. Naval Research Laboratory.

References

1. Ng FM, Ritchie JM, Simmons JEL, Dewar RG (2000) J Mater Process Technol 107:37
2. Akovali G, Bernardo CA, Leidner J, Leszek AU, Xanthos M (eds) (1998) Frontiers in the science and technology of polymer recycling. Kluwer Academic Publishers, Dordrecht
3. Brandrup J, Bittner M, Michaeli W, Menges G (eds) (1996) Recycling and recovery of plastics. Hanser Gardner Publications
4. Brebu M, Vasile C, Antonie SR, Chiriac M, Precup M, Yang J, Roy C (2000) Polym Degrad Stabil 67:209
5. Emanuelsson V, Simonson M, Gevert T (2007) Fire Mater 31:311
6. Kim C, Jin Z, Jiang P, Zhu Z, Wang G (2006) Polym Test 25:553
7. Kim C, Jin Z, Huang X, Jiang P, Ke Q (2007) Polym Degrad Stabil 92:537

8. Kobayashi K, Nakayama S, Niwa T (1994) Proceedings of the fourth international conference on properties and applications of dielectric materials, p 678
9. Kujirai T, Akagira T (1925) Sci Pap Inst Phys Chem Res 2:223
10. Mazzanti G, Montanari GC, Simoni L (1997) IEEE Electric Insulat Mag 13:24
11. Takeda K, Amemiya F, Kinoshita M, Takayama S (1997) J Appl Polym Sci 64:1175
12. Benes M, Placek V, Matuschek G, Kettrup A, Gyoryova K, Balek V (2006) J Appl Polym Sci 99:788
13. Chen N, Wan C, Zhang Y, Zhang Y (2004) Polym Test 23:169
14. Pita VJRR, Sampaio EEM, Monteiro EEC (2002) Polym Test 21:545
15. Wang Y, Cheng S, Li W, Huang C, Li F, Shi J (2007) Polym Bull 59:391
16. Kubo K, Masamoto J (2002) J Appl Polym Sci 86:3030
17. Hay AS, Blanchard HS, Endres GF, Eustance JW (1959) J Am Chem Soc 81:6335
18. Hay AS (1967) Adv Polym Sci 4:496
19. White DM, Klopfer HJ (1972) J Polym Sci A 1(10):1565
20. Kleiner LW, Karasz FE, Macknight W (1979) J Polym Eng Sci 19:519
21. Gang H, Lining Y, Hongxin C (1999) Appl Eng Plast 12:19
22. Heijboer J (1968) J Polym Sci C 16:37
23. Karasz FE, O'Reilly JM (1965) Polym Lett 3:561
24. Jachowicz J (1978) J Appl Polym Sci 22:2891
25. Chandra R (1982) Prog Polym Sci 8:469
26. Caddell RM, Bates T, Yeh G (1972) Mater Sci Eng 9:223
27. Sweeney J, Caton-Rose P, Coates PD (2002) Polymer 43:899
28. Sweeney J, Caton-Rose P, Coates PD, Unwin AP, Duckett RA, Ward IM (2002) Int J Plast 18:399
29. Parsons EM, Boyce MC, Parks DM, Weinberg M (2005) Polymer 46:2257
30. Dasari A, Misra RDK (2003) Mater Sci Eng 358:356
31. G'Sell C, Jonas JJ (1979) J Mater Sci 14:583. doi:10.1007/BF00772717
32. G'Sell C, Hiver JM, Dahoun A, Souahi A (1992) J Mater Sci 27:5031. doi:10.1007/BF01105270
33. G'Sell C, Hiver JM, Dahoun A (2002) Int J Solids Struct 39:3857
34. Buisson G, Ravi-Chandar K (1990) Polymer 31:2071
35. Parsons EM, Boyce MC, Parks DM (2004) Polymer 45:2665
36. Fang QZ, Wang TJ, Li HM (2006) Polymer 47:5174
37. Xiao X (2008) Polym Test 27:284
38. Kurtz SM, Pruitt L, Jewet CW, Crawford RP, Crane DJ, Edidin AA (1998) Biomaterials 19:1989
39. Kausch HH, Gensler R, Grein CH, Plummer CJG, Scaramuzzino P (1999) J Macromol Sci Phys B 38:803
40. Inagaki K, Ekh J, Zahrai S (2007) Int J Solids Struct 44:1657
41. Nair SV, Wong SC, Goettler LA (1997) J Mater Sci 32:5335. doi:10.1023/A:1018618912039
42. Dean G, Read B (2001) Polym Test 20:677
43. Rees DWA (2000) Mechanics of solids and structures. Imperial College Press, London
44. Kang KW, Goo BC, Kim JH, Kim HS, Kim JK (2007) Key Eng Mater 353–358:142
45. Ivanov SS, Ivanov ES (1976) Fiziko-Khimicheskaya Mekhanika Materialov 12:106
46. Shiao ML, Nair SV, Garrett PD, Pollard RE (1994) Polymer 35:306
47. Friedrich K (1985) Compos Sci Technol 22:43